

Direct determination of the reaction path of Sb_4 on $\text{Si}(001)$ with scanning tunneling microscopy

Y. W. Mo

IBM Research Division, Thomas J. Watson Research Center, Yorktown Heights, New York 10598

(Received 2 June 1993)

The complex reaction path of the dissociative chemisorption of Sb_4 on $\text{Si}(001)$ involving four distinct types of precursor states is determined using a direct "tracking" method with scanning tunneling microscopy. The energy barriers and the prefactors for the transitions between different states are measured by analyzing the population distribution of Sb clusters as a function of thermal treatment. These precursors are found not to have thermal mobility before dissociation, contrary to the widely held notion about precursor states.

I. INTRODUCTION

The reaction dynamics of molecules with solid surfaces is an important issue in surface science. It has long been known that molecular chemisorption on solid surfaces often involves intermediate precursor states.¹ Many studies have been conducted to determine the reaction path for different molecules on different solid surfaces.² The principal methods of past studies of precursors have been spectroscopy with macroscopic spatial resolution and molecular-beam experiments. Because of the indirectness of these methods, it is extremely difficult to identify the precursor states and to measure the conversion kinetics for a system that involves more than one precursor state. As a consequence, a single precursor state has often been assumed in the interpretation of data from these studies. Scanning tunneling microscopy (STM), because of its atomic resolution, allows direct identification of precursor states and quantitative measurement of their conversion kinetics.

There is great interest in understanding the reaction path of dopant molecules with semiconductor surfaces,³⁻¹⁰ because many common dopants are deposited in molecular form, such as Sb_4 and As_4 . The interactions of dopant molecules with semiconductor surfaces determine the incorporation coefficient of the dopants in the semiconductor films. In particular, the stability and mobility of dopant precursors determine the quality of the δ -doping structures.¹¹

In a previous STM study,¹² we have reported the identification of four distinct types of precursors in the dissociative chemisorption of Sb_4 on $\text{Si}(001)$. Because of its complexity, the reaction path was not fully determined but only an effective energy barrier was obtained for the overall conversion of all precursors to the final state. In the present study, the detailed path of this complex reaction is determined by a "tracking" method that allows us to follow individually the thermally induced changes in each Sb_4 cluster. In addition, the energy barriers and prefactors for the specific conversions between different precursors are measured. Contrary to the popular perception,^{2,6} we also find that these precursors have no thermal mobility before dissociation.

II. EXPERIMENT

Experiments were carried out in an ultrahigh vacuum chamber with a base pressure of 4×10^{-11} torr, containing a STM and an Sb Knudsen cell. At typical operating temperatures between 500 and 700 K, Sb evaporates nearly exclusively as Sb_4 with the partial pressures of other species being less than 1% of the total.¹³ The sample is cleaned by direct-current heating at 1527 K for several seconds, and is then allowed to cool down to room temperature (RT) for Sb deposition. All STM scans are taken at RT. The temperature for cleaning the sample is measured using a disappearing-filament pyrometer, while the lower temperatures used for thermal conversion of Sb_4 clusters are measured with a W 5% Re/W 26% Re thermocouple. The overall uncertainty in the temperature measurement is estimated to be ± 10 K, including the temperature drift during the annealing period.

One crucial step in determining the detailed reaction path is the tracking experiment in which the same Sb clusters are imaged before and after thermal annealing. During annealing, the STM tip is withdrawn from the sample surface by about 100 μm . To be able to come back to image exactly the same area requires high stability of the STM against thermal cycling. This is achievable because of the rigid STM design such that mechanical shift caused by thermal annealing is almost fully reversed after cooling down to RT. The large scan range ($\sim 5 \mu\text{m}$) of the STM also allows a large tolerance for the residual shift which is typically less than 0.2 μm in both the x and y directions.

III. RESULTS AND DISCUSSION

After deposition at RT of a small fraction, e.g., 0.02, of a monolayer of Sb_4 , Sb clusters are observed on $\text{Si}(001)$. Close examination reveals that there are five distinct types of Sb clusters, each consisting of four Sb atoms, as shown in Fig. 1. Because the optimal resolution for different types of clusters is obtained with different bias voltages, images at two different biases are shown [Figs. 1(a) and 1(b)]. The final-state cluster (labeled E) consists of two dimers with the dimer bonds perpendicular to the Si dimer bonds in the substrate, consistent with past stud-

ies of the equilibrium structure of the Sb layer on Si(001) formed at elevated temperatures.⁷ The remaining four types are precursors that form the pathway for the Sb₄ molecules to reach the final state (*E*) of dissociative

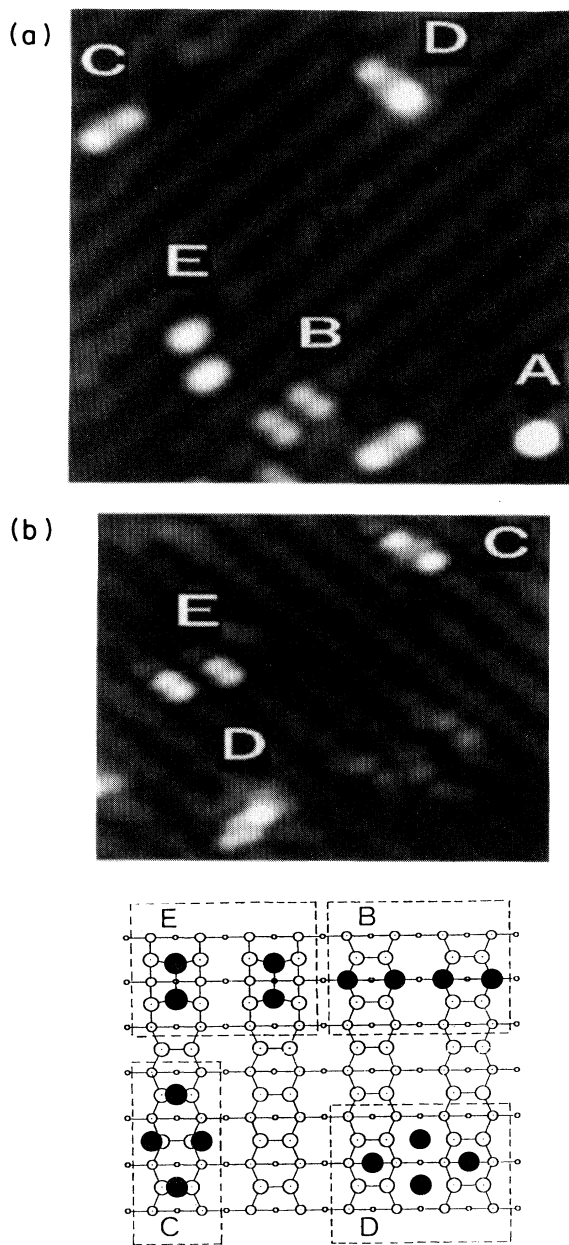


FIG. 1. STM images of Sb₄ clusters on Si(001) deposited at room temperature. Both are taken with a tunneling current of 0.2 nA. (a) Five types of clusters: one "ball" (*A*), one "rotated dimer" (*B*), two "dumbbells" (*C*), one "rotated dumbbell" (*D*), and one final-state cluster (*E*). Image area is 70×80 Å. For the tip bias of +1.0 V, four Sb atoms are resolved in *B* clusters. (b) With a tip bias of +0.7 V, four atoms in each of three types (*C*, *D*, and *E*) of clusters can be seen. Image area is 70×60 Å. (c) Schematic models for the likely configurations of the four types of clusters. Filled circles are Sb atoms and the largest open circles are the top-layer Si atoms.

chemisorption. These precursors have very distinctive configurations. Type *A* appears as a ball without any resolvable internal features, appearing much higher (brighter in the STM images) than the other types, and is always located on top of the substrate dimer rows. We call them "ball" clusters. We believe that they still retain a more or less three-dimensional structure, similar to that of the tetrahedral molecules in the gas phase. Type *B* consists of a pair of dimers, but the dimer bonds are parallel to those of the substrate dimers, unlike those of the final-state cluster. They are called "rotated dimers." The other two types have two pronounced peaks with two weaker ones in between. We call the one with the long axis parallel to the substrate dimer rows "dumbbells" (*C*), and the one with the long axis perpendicular to the substrate dimer rows "rotated dumbbells" (*D*). The rotated dumbbells all appear tilted with one end higher than the other. Figure 1(c) contains schematic drawings of likely configurations for the four cluster types. No model is shown for the ball cluster because there is not much information from the STM except its apparent height. We caution that the details in these sketches should not be taken as a final determination of the atomic structures, because with STM alone we cannot unequivocally determine the structural details of the Sb clusters.

At RT, all Sb clusters formed after deposition are structurally stable and spatially immobile. However, as reported previously,¹² all four precursors (*A*, *B*, *C*, and *D*) can be converted to the final state (*E*) either through a STM tip-induced conversion process or by thermal annealing.

In order to study the kinetics of the thermal conversion of the precursors, we measure the average population distribution of the Sb clusters as a function of the thermal treatment. This is achieved by simply counting the Sb clusters in a large number of STM images obtained after thermal annealing and subsequent quenching to RT. Figure 2 shows the time evolution of the population distribution of Sb clusters as annealed at 345 K from 0 to 80 min. The typical number of each cluster type at every data point is several hundred, except for the cluster type that has nearly diminished. Several observations can be made from the plot. First, the initial population distribution among the five cluster types after RT deposition is rather uniform. Because these clusters are formed at the moment of condensation of Sb₄ on Si(001), we speculate that the exact impact point and/or the molecular orientation of Sb₄ at the moment of landing determines this population distribution.¹⁴ It could also be affected by the different vibrational modes of Sb₄ excited by the energy of condensation.¹⁵ Second, with increasing annealing time the population of the *E* clusters grows steadily at the expense of the others, suggesting that it is the most stable state. Actually, after sufficiently long annealing at all temperatures of experiment, the population of the type-*E* cluster reaches 100% within the experimental uncertainty. This indicates that the type-*E* structure is the final state of the dissociative chemisorption of Sb₄ on Si(001), consistent with the previous studies by STM and other techniques.⁷⁻¹⁰ The behavior of other clusters, however,

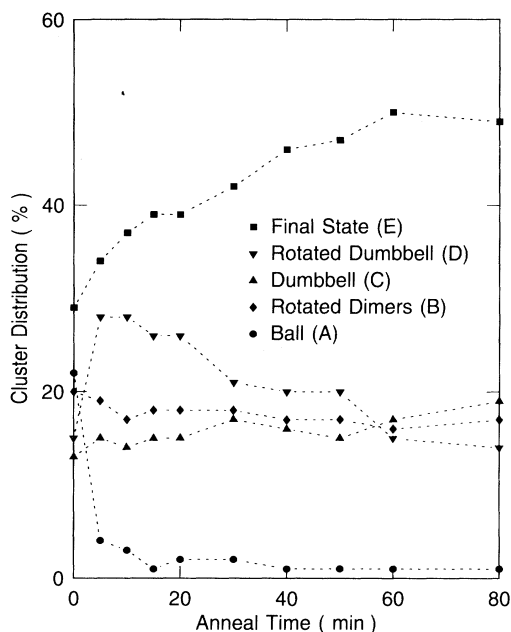


FIG. 2. The population distribution of the Sb clusters as a function of the annealing time at 345 K. The starting point corresponds to the initial distribution after room-temperature deposition. The uncertainty of the data is estimated to be 2–3 % of the total population.

varies significantly. The ball cluster (*A*) is obviously the least stable precursor and its population decreases rapidly from 21% to 5% after the first anneal of 5 min. Upon further annealing its population decays to practically zero within the uncertainty of the data. Meanwhile, the evolution of the *D* population shows a peak. This suggests that at least some balls (*A*) go through rotated dumbbells (*D*) to reach the final state. Because of the high initial ball population, during the early time of the annealing there are more conversions from *A* to *D* than the decay of *D* and hence its population rises temporarily. When the population of *A* is nearly diminished the population of the *D* cluster starts to decay. The population of the *B* cluster also shows a slight increase during the annealing at this temperature. This indicates that it is also an intermediate step for the conversion to the final state of some other precursors.

Although some qualitative conclusions can be made from the above measurements of the average population distribution, it is difficult to obtain quantitative results for the conversion parameters because of the complexity of this reaction path. Because there are five different types of Sb clusters and there could be conversions between any two of them, a rate equation with 20 unknowns is needed to describe the reaction process at each temperature. Clearly, it is nearly impossible to solve this rate equation if we do not have another nonaveraging method that directly determines the reaction path and thus allows us to eliminate most of the 20 parameters in the rate equation. The tracking experiment provides such a direct means.

In a tracking experiment, we image the same Sb clus-

ters before and after a cycle of thermal annealing at a certain temperature. During the annealing, the STM tip is withdrawn from the sample surface to eliminate any possible tip-induced conversion of Sb precursors. This image-anneal-image method is similar to that used in surface diffusion studies by field-ion microscopy.¹⁶ This STM method allows us to follow directly the reaction path of individual Sb clusters while avoiding the potential influence of the STM tip. An alternative way to directly monitor the changes of individual clusters is to image while keeping the sample at a suitable temperature. The potential concern for this method, however, is that the STM tip may cause nonthermal conversions which is difficult to separate from the thermal ones. Because the STM tip can induce conversions in the Sb precursors at RT with a higher tip bias,¹² it is likely that if scanning at elevated temperatures, the STM-tip effect is *not* negligible even if a low bias, e.g., 1.0 V, is used, whereas in the tracking method used here, the cluster conversion due to thermal annealing and the STM observation are temporally separate and hence tip effect can be avoided.

An example of the tracking experiment is shown in Fig. 3 in which four ball clusters (*A*) are converted by thermal annealing. The statistics of the conversion products of 200 balls is listed in Table I. Several observations can be made. First, a majority of the balls (66%) are converted to rotated dumbbells (*D*), in agreement with the qualitative conclusion from the average measurements in Fig. 2. At the same time about 6% are converted to rotated dimers (*B*) and 6% to the final state (*E*). Actually, the conversion from *A* to *B* and *E* is due to the subsequent conversion of the *D* clusters generated from the *A* clusters, because the tracking experiment for the *D* clus-

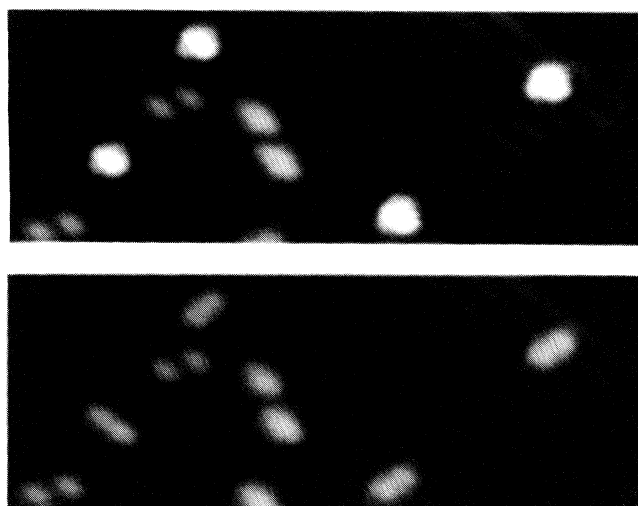


FIG. 3. STM images of the same Sb clusters before and after annealing at 345 K for 5 min. (a) Before annealing. Four balls (*A*) are observed, appearing higher than the other types of clusters. Due to a less sharp STM tip, the balls appear not to be perfectly round and the other types of Sb clusters are also not as well resolved as those shown in Fig. 1. (b) After annealing. The four balls are all converted: three to rotated dumbbells (*D*) and one to the final state (*E*). Note that there is no displacement and desorption of the clusters during the conversion.

TABLE I. The percentage distribution of the conversion products of 200 balls (*A*) after thermal annealing at 345 K for 5 min, as measured from the "tracking" experiment in which the changes in individual clusters are identified after annealing.

Rotated dumbbell	Unchanged	Rotated dimer	Final state	Dumbbell
(<i>D</i>)	(<i>A</i>)	(<i>B</i>)	(<i>E</i>)	(<i>C</i>)
66%	22%	6%	6%	0

ters shows that after the same annealing period about 10% of the *D*'s are converted to the *B* and 10% to *E*. Another interesting point is that no balls (*A*) are converted to the dumbbells (*C*). Furthermore, from the tracking experiments at several temperatures, we observe no conversions from *any* types of clusters to the dumbbells (*C*). Therefore the dumbbells are only created at the moment of the condensation of the Sb_4 on the surface. The fact that the balls cannot convert to the dumbbells is somewhat counterintuitive in terms of their configurations: both *A* and *C* are located on top of the substrate dimer rows while a *D* cluster bridges two substrate dimer rows. One might imagine that the conversion within a single dimer row should be the easier path.

The tracking experiments further indicate that the primary decay path for both *C* and *D* clusters is through the *B* cluster, consistent with the result of the average measurement of Fig. 2 where the *B* population rises as a function of annealing time at 345 K. The tracking experiment also shows that some of the *C* and *D* clusters convert to the final state (*E*). Currently, however, we cannot determine unequivocally whether or not these conversions are due to the subsequent conversion from the *B* clusters generated by the *C* and *D* clusters. It is nevertheless clear that the direct channel from *C* or *D* to the final state, if existing, is rather weak. Figure 4 summarizes the above information into a graphic depiction of this multistage reaction path.

As shown in Fig. 3, another important observation from the above tracking experiment is that all of the precursors convert without any displacement, i.e., these precursors have no thermal mobility.¹⁷ This is contrary to the widely held notion about the precursor states.^{2,6} Furthermore, at least at the temperatures of all tracking experiments (< 573 K), there is no desorption of any *Sb* clusters during thermal conversion. The tracking experiment allows us to obtain direct and unambiguous comparison of the rates of conversion, diffusion, and desorption of precursors which are the basic parameters for molecule-surface interactions. A full understanding of the general relationship among them should shed light on the interaction between adsorbate and substrate, and that between the adsorbates themselves.

Having determined the reaction path with the tracking method, we can greatly simplify the rate equation for this reaction path. Because there is no conversion from any other type of cluster to either *A* or *C*, their population follows the simple function of a first-order decay, described by

$$N = N_0 e^{-\lambda t},$$

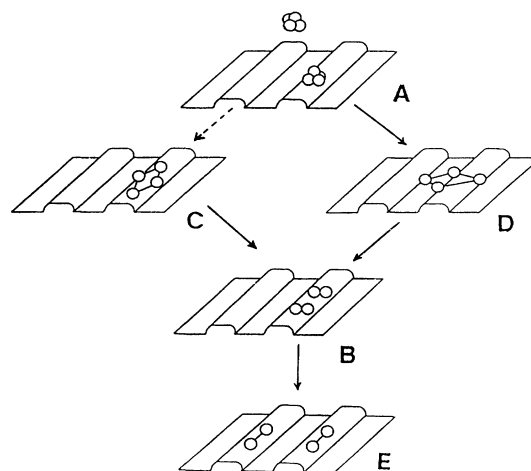


FIG. 4. Schematic illustration of the reaction path of Sb_4 on $\text{Si}(001)$. The ridges represent the substrate dimer rows. For simplicity, the atomic structure of the substrate is not shown. The dashed line between the *A* and *C* sections indicates that there is no thermal transition between *A* and *C*, and *C* is created only at the moment of condensation.

where N is the population at time t , N_0 is the initial population, and λ is the conversion rate at temperature T . Therefore the decay rate for either *A* or *C* can be easily obtained from any two data points in plots like Fig. 2. The population evolution of the *D* cluster, however, does not follow such a simple form because its population is coupled to that of the balls (*A*). To avoid this complication, we compute the decay rate of *D* using a pair of data points after the population of the balls has nearly diminished. After this time the population decay of the rotated dumbbells (*D*) becomes approximately first order, following Eq. (1).

Using the above method, the conversion rates for the balls, dumbbells, and rotated dumbbells are measured at several different temperatures, as shown in Fig. 5 in Arrhenius plots. From a least-squares fit, we obtain the energy barrier and the prefactor for a ball cluster to convert to a rotated dumbbell 0.7 ± 0.1 eV and $\sim 10^8$ sec^{-1} , respectively; those for a rotated dumbbell to convert to a rotated dimer 0.9 ± 0.1 eV and $\sim 10^9$ sec^{-1} , respectively; and those for a dumbbell to convert to a rotated dimer 0.8 ± 0.1 eV and $\sim 10^7$ sec^{-1} , respectively.

If we believe that a ball cluster still retains a more or less molecular structure, we can categorize the 0.7-eV energy barrier for the conversion of *A* to *D* as that from a so-called molecularly chemisorbed² state to a more two-dimensional structure (*D*). The next step in the conversion from either *D* or *C* to *B* can be considered as a dissociation process because the rotated dimers (*B*) consist of two independent units (two dimers) each of which is free to change its orientation into the final state. In order to break either *C* or *D* into two separate dimers (either *B* or *E* type) at least two *Sb-Sb* bonds need to be broken. Therefore the small energy barriers measured here suggest a concerted motion that provides a low barrier path.

The conversion rate of the rotated dimers to the final

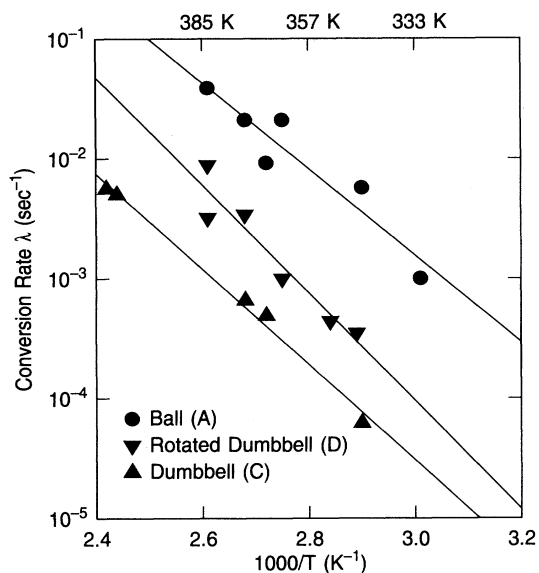


FIG. 5. The conversion rates of three types (*A*, *C*, and *D*) of Sb clusters as a function of the temperature. The slope and the intercept of the least-squares fit give the energy barriers and the prefactors for the conversion, respectively.

state involves a different complication because reversed conversions from the final state (*E*) back to the rotated state (*B*) are also observed.¹⁸ In other words, an isolated Sb dimer on $\text{Si}(001)$ can be reversibly rotated back and forth between two orthogonal orientations. This indicates that the energy difference between the two states is not very large, although the final-state energy is still lower than that of the rotated dimer. As a consequence, the conversion rate from the above measurements is only a lower limit. More work is underway to measure the energy difference between the two dimer orientations as well as the energy barrier between the two states.

IV. CONCLUSIONS

We have determined, using a direct tracking method with the STM, the reaction path of the dissociative chemisorption of Sb_4 on $\text{Si}(001)$ which involves four distinct types of precursor states. Combined with the measurements of the average population distribution of Sb clusters as a function of thermal treatment, the energy barriers and the prefactors for conversions between different states are obtained. These precursors are found to have no thermal mobility before dissociation, contrary to the popular notion about precursor states. These results indi-

cate that the reaction of molecules with solid surfaces can be extremely complex and much work is needed to achieve a comprehensive understanding for the adsorption kinetics of even a simple molecule such as Sb_4 .

Finally, studying the reaction path of molecules on surfaces with the STM has unique advantages. First it allows direct identification of different types of coexisting precursors. Second, direct measurements of the conversion rates are less model dependent than the conventional molecular-beam method.

In particular, the tracking method used in this study to determine the reaction path is useful for studying various kinetic processes. Because the STM can image exactly the same area before and after thermal annealing, it allows one to track directly the changes in the cluster configuration or surface morphology at the atomic scale. Compared to the alternative method of real-time imaging at elevated temperatures, the tracking method of image-anneal-image has certain advantages. First, it avoids potential tip-induced events because the changes in clusters due to thermal annealing only occur in the absence of the STM tip. For Sb_4 on $\text{Si}(001)$, this is obviously important because the tip is known to be able to induce the conversion of Sb_4 precursors, but it could also be important for other systems as well. In real-time observations, STM images are taken while thermal changes are occurring at a rate adequate for the STM to follow, which means that the thermal energy is nearly sufficient to induce changes. Therefore, even a small perturbation from the STM tip could have large effects on the conversion rates. Second, the tracking method has a larger dynamic range in time than that of real-time scans because in the tracking experiment the observation is decoupled from the thermal conversion and there is no need to match the time scale of the two processes whereas in the real-time observations the rate of thermal change needs to match the STM scan rate.

We believe that the STM method for studying the conversion kinetics of precursors is applicable to many other systems. The knowledge on the atomic configuration, the stability, and the mobility of precursor clusters thus obtained should provide useful input for theoretical studies of a reaction path of molecules on solid surfaces.

ACKNOWLEDGMENTS

The author would like to thank R. Tromp, J. Demuth, R. Walkup, M. Yu, and B. Swartzentruber for valuable discussion, and P. Yuan for help in numerical treatment of the data.

¹I. Langmuir, *Chem. Rev.* **6**, 451 (1929).

²For a review, see, e.g., *Kinetics of Interface Reactions*, edited by M. Grunze and H. J. Kreuzer (Springer-Verlag, Berlin, 1987).

³C. T. Foxon and B. A. Joyce, *Surf. Sci.* **40**, 434 (1975).

⁴R. A. Metzger and F. G. Allen, *Surf. Sci.* **137**, 397 (1984).

⁵D. Rich, G. E. Franklin, F. M. Leibsle, T. Miller, and T.-C. Chiang, *Phys. Rev. B* **40**, 11 804 (1989).

⁶S. A. Barnett, H. F. Winters, and J. E. Greene, *Surf. Sci.* **165**,

303 (1986).

⁷J. Nogami, A. A. Baski, and C. F. Quate, *Appl. Phys. Lett.* **58**, 475 (1991).

⁸R. D. Brigans, D. K. Biegelsen, and L.-E. Swartz, *Phys. Rev. B* **44**, 3054 (1991).

⁹W. F. J. Slijkerman, P. J. Zagwijn, and J. F. van der Veen, *Surf. Sci.* **262**, 25 (1992).

¹⁰E. B. Elswijk and E. J. van Loenen, *Ultramicroscopy* **42-44**,

- 884 (1992).
- ¹¹J. C. Bean, *Appl. Phys. Lett.* **33**, 654 (1978).
- ¹²Y. W. Mo, *Phys. Rev. Lett.* **69**, 3643 (1992).
- ¹³R. Hultgren, R. L. Orr, P. D. Anderson, and K. K. Kelly, *Selected Values of Thermodynamic Properties of Elements* (Wiley, New York, 1973), p. 448.
- ¹⁴P. J. Feibelman, *Phys. Rev. Lett.* **67**, 461 (1991); B. Hammer, K. W. Jacobsen, and J. K. Nørskov, *ibid.* **69**, 1971 (1992).
- ¹⁵L.-S. Wang, B. Niu, Y. T. Lee, D. A. Shirley, E. Ghelichkhani, and E. R. Grant, *J. Chem. Phys.* **93**, 6318 (1990).
- ¹⁶E. W. Muller and T. T. Tsong, *Field Ion Microscopy Principles and Applications* (American Elsevier, New York, 1969).
- ¹⁷In a separate experiment, it is shown that these precursors also do not have transient mobility at the moment of condensation; Y. W. Mo (unpublished).
- ¹⁸Y. W. Mo, *Science* **261**, 886 (1993).

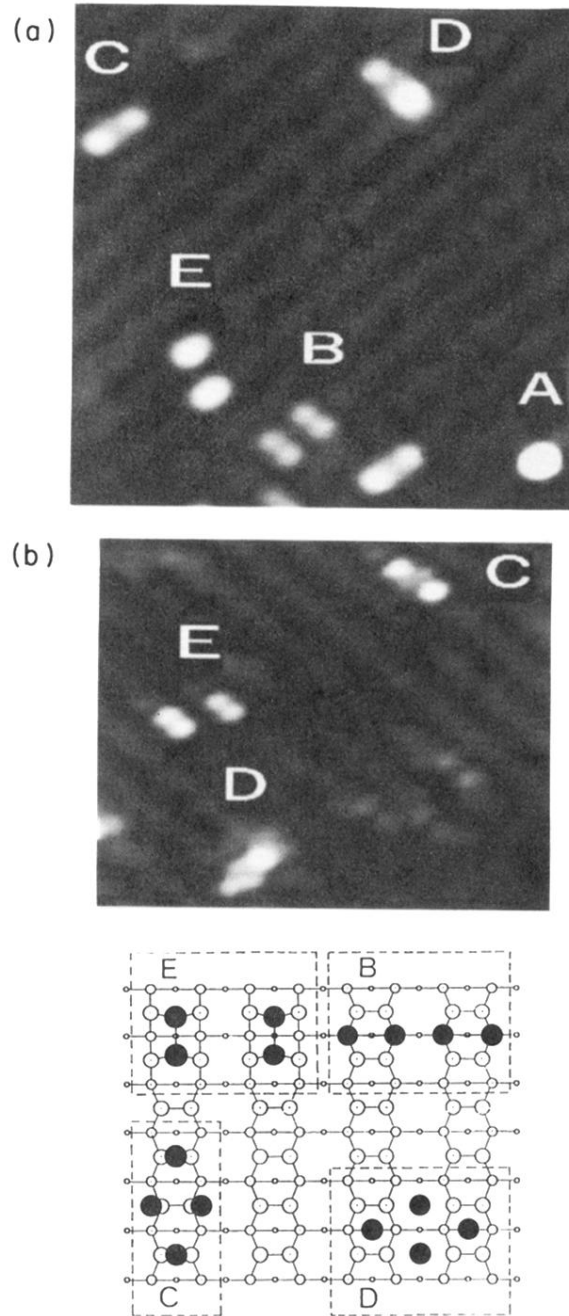


FIG. 1. STM images of Sb_4 clusters on $\text{Si}(001)$ deposited at room temperature. Both are taken with a tunneling current of 0.2 nA. (a) Five types of clusters: one “ball” (A), one “rotated dimer” (B), two “dumbbells” (C), one “rotated dumbbell” (D), and one final-state cluster (E). Image area is $70 \times 80 \text{ \AA}$. For the tip bias of +1.0 V, four Sb atoms are resolved in B clusters. (b) With a tip bias of +0.7 V, four atoms in each of three types (C , D , and E) of clusters can be seen. Image area is $70 \times 60 \text{ \AA}$. (c) Schematic models for the likely configurations of the four types of clusters. Filled circles are Sb atoms and the largest open circles are the top-layer Si atoms.

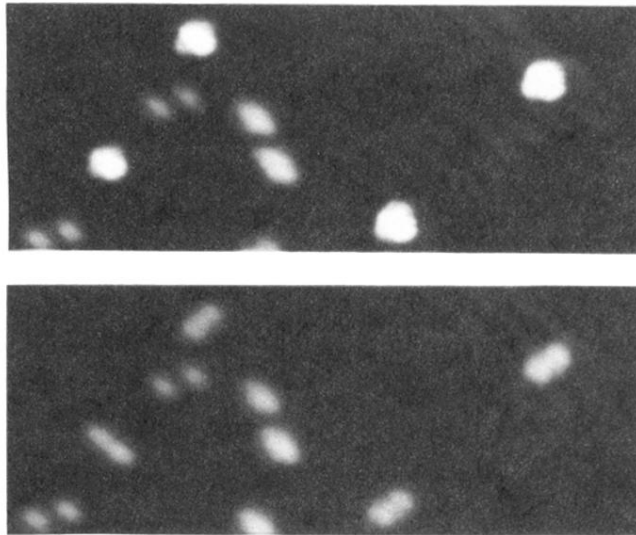


FIG. 3. STM images of the same Sb clusters before and after annealing at 345 K for 5 min. (a) Before annealing. Four balls (*A*) are observed, appearing higher than the other types of clusters. Due to a less sharp STM tip, the balls appear not to be perfectly round and the other types of Sb clusters are also not as well resolved as those shown in Fig. 1. (b) After annealing. The four balls are all converted: three to rotated dumbbells (*D*) and one to the final state (*E*). Note that there is no displacement and desorption of the clusters during the conversion.